Journal of
Polymer & Composites

https://journals.stmjournals.com/jopc

ISSN: 2321-2810 (Online)
ISSN: 2321-8525 (Print)
Volume 14, Special Issue 2, 2026
DOI (Journal): 10.37591/JoPC

Research JoPC

Improvement of Geometric Tolerances and Mechanical Properties of Aluminum Hybrid Metal Matrix Composites

Lokanadham Dharmana[1], K. DurgaPrasad[2], Duppala Azad[3], B. Roop Sandeep[4], D. Bhanuchandra Rao[5,*], S. Hari Prasad[6]

Abstract

In the field of metal matrix composite materials, there has been a generous thrust towards the development of electrical discharge machining (EDM). In this study, stir casted aluminum hybrid metal matrix composites were successfully machined using EDM by analyzing the input process parameters namely, pulse-on time, peak current, and gap voltage using L27 orthogonal array. The ideal conditions for various output responses such as material removal rate, circularity, and radial overcut were examined by employing grey relational analysis procedure by optimizing the various input process parameters. A response table was generated utilizing grey relational grading to determine the optimal individual parameter settings. From the ANOVA table, results highlighted the pivotal role of the current parameter, contributing 53.183% to overall performance. Optimal conditions identified included a peak current of 14.5 A, a pulse-on time of 50 µs, and a gap voltage of 45 V. Validation tests confirmed substantial improvements compared to initially predicted parameters. The machined surfaces were analyzed using mechanical testing methods, and observed maximum ultimate strength, hardness and wear resistance for the base material reinforced with 6 wt.% of titanium carbide (TiC), and 2 wt.% of boron nitrides (BN). The circularity and radial overcut of the machined surface distended with an increase in peak current throughout its range. The MRR deviation was increased with a combination of elevated peak current and lower pulse-on time.

Keywords: AMCs, TiC, BN, EDM, GRA, mechanical and tribological properties

INTRODUCTION

A prominent class of materials that has attracted a lot of interest in the fields of materials science and engineering were metal matrix composites (MMCs). Among MMCs, Aluminum hybrid metal matrix composites (AHMMCs) stand out as particularly promising due to their unique combination of properties and versatility. The project aimed at exploring and enhancing the mechanical properties and geometric tolerances of AHMMCs, it is essential to provide a comprehensive introduction to these materials and their significance in contemporary engineering applications [1–3]. Aluminum, with its low density, excellent corrosion resistance, and favorable mechanical properties, serves as a preferred matrix material in many MMCs. When combined with reinforcing phases such as ceramics, carbides, or nanoparticles, AHMMCs that exhibit superior mechanical performance compared to monolithic aluminum

*Author for Correspondence
D. Bhanuchandra Rao

[1-5]Assistant Professor, Department of Mechanical Engineering, Aditya Institute of Technology and Management, Tekkali, Andhra Pradesh, India
[6]Assistant Professor, Department of Physics, BS&H, Aditya Institute of Technology and Management (AITAM), Tekkali – 532201, Srikakulam, Andhra Pradesh, India.

Received Date: November 13, 2025
Accepted Date: November 25, 2025
Published Date: April 17, 2026

Citation: Lokanadham Dharmana, K. DurgaPrasad, Duppala Azad, B. Roop Sandeep, D. Bhanuchandra Rao, S. Hari Prasad. Improvement of Geometric Tolerances and Mechanical Properties of Aluminum Hybrid Metal Matrix Composites. Journal of Polymer & Composites. 2026; 14(Special Issue 2): S1583–S1592p.

alloys. The accumulation of ceramic particles is easy in the handling of aluminum metal matrix composites (AMMCs). Additionally, the accretion of secondary particulate reinforcement like Al_{2O3}, graphite, and Boron Nitride (BN), as well as the accumulation of particulate reinforcement like B_4C, SiC, TiC, Al_{2O3}, Si_3N_4, and ZrB_2, improves the mechanical and thermal properties of AMMCs. The AMMCs' tribological characteristics exhibited distension [4–7]. The most influential parameters affecting performance measures are current and pulse-on time. Researchers identified optimal parameter settings using the Taguchi technique to maximize performance. Mathematical modelling has been developed to predict optimal conditions for Electric Discharge machining(EDM). However, despite the progress in EDM research, there remains an open area of investigation, particularly concerning matrix phase reinforcement with multiple particulates. Most studies have focused on single particulate reinforcement, leaving room for exploration in this domain. In this research, we aim to fill this gap by investigating EDM machining on matrix phase reinforced with two particulates [8–11]. Senthilkumar et al. [12]used grey relational analysis for optimization to compare the effects of input factors on machining performance. Circularity, cylindricity, and radial overcut were significantly impacted by peak current, pulse duration, and gap voltage; further information was obtained by SEM surface analysis. The wear resistance of AA6351 aluminum matrix composites supplemented with 5 weight percent SiC and 5 weight percent B_4C by mix casting was compared by Thirumalai et al. [13]. Protective layer formation between surfaces in contact, especially under loads of up to 60 N and sliding velocities between 1 and 3 m/s, resulted in improved wear resistance. Using response surface methods, Hourmand et al. [14] investigated in situ EDM of Al–Mg_2Si composites. ANOVA confirmed that the primary determinants of material removal rate (MRR) were voltage, current, and their interaction. Despite the extensive literature on optimization methodologies in machining processes, limited effort has been directed towards optimizing geometric tolerances, particularly in the realm of hybrid metal matrix composites. Grey Relational Analysis (GRA) is used in this study to optimize EDM settings for AH-MMCs in order to improve radial overcut (ROC), material removal rate (MRR), and circularity (CR). EDM machining and stir casting were used to create AH-MMCs. An L27 orthogonal array was used to assess the gap voltage (V), peak current (I), and pulse-on time (POT). ANOVA identified the most significant factor, whereas GRA produced the ideal settings for improved performance. The optimal configurations and improvements in grey relationship grade were validated by confirmation tests. The impact of peak current and pulse-on time on machining performance was further investigated using surface plots.

MATERIALS AND METHODOLOGY

Aluminum alloy 7075, an aerospace-grade material renowned for its exceptional strength and toughness, is mostly made up of aluminum, with zinc serving as the main alloying element. Tiny amounts of magnesium, copper, and chromium are added as supplements [15, 16]. Its strength can be further augmented through heat treatment processes, enhancing its mechanical properties. The chemical composition has shown in Table 1.

Titanium Carbide (TiC) is selected as one of the reinforcing materials for its exceptional hardness and wear resistance properties. TiC is renowned for its remarkable hardness, making it one of the hardest materials known. This property enables TiC to effectively strengthen the Aluminum hybrid metal matrix composites (Al-HMMCs) and enhance their resistance to wear, abrasion, and mechanical deformation. TiC has a high melting point of approximately 3200°C, ensuring stability during processing and service conditions. By uniformly dispersing mechanical stresses and preventing corrosion, it improves the composite's mechanical qualities and longevity [17–19]. Boron Nitride (BN) is another reinforcing material chosen for its unique properties that contribute to the enhancement of Al-HMMCs. BN is characterized by its exceptionally high thermal conductivity, facilitating efficient heat dissipation and thermal management within the composite material [20, 21].

Table 1. AA7075 chemical composition.

Zn	Mg	Cu	Fe	Si	Mn	Al
6.2	2.0	1.7	0.5	0.4	0.5	Bal.

Fabrication of Composite

To make the composite basis, scrap aluminum alloy (7075) was cast in a furnace. To prevent oxidation, reinforcements containing 6 weight percent TiC and 2 weight percent BN were warmed to 1000°C. Before being cooled to the liquidus temperature, the alloy was heated above the melting point to the liquidus stage. To get rid of contaminants, a degasser and cover-all powder were applied. To ensure a uniform dispersion, heated reinforcements were added to the molten alloy and physically agitated for five to ten minutes at 3500 rpm. A homogenous aluminum hybrid metal matrix composite was produced by casting the molten mixture in a 100 × 100 × 10 mm heated die and allowing it to harden.

Machining Techniques

For the machining process, we utilize a die-sinking Electrical Discharge Machining (EDM, vide in Fig.1a) system equipped with a three-phase servo stabilizer. With the workpiece on positive and the electrode on negative polarity, a copper electrode measuring 10 mm by 100 mm is used Figure 1(b). In order to fully fill the closed machine bed and submerge the electrode and workpiece in it for efficient machining, EDM oil is utilized as the dielectric fluid at a rate of 1.0 kgf/cm².

The objective is to improve the geometric tolerances of Al-HMMCs, including circularity, material removal rate, and radial overcut, to meet stringent application requirements. Rigorous quality assurance measures, including in-process inspections and dimensional measurements using coordinate measuring machines (CMM), are implemented to ensure integrity and accuracy throughout the machining process. Additionally, the EDM machine setup, with appropriate parameters like gap voltage, pulse-on time, and peak current plays a crucial role in achieving desired outcomes in terms of material removal rates, surface finish, and dimensional accuracy. Based on prior research and preliminary experimentation, identifying the key EDM parameters that significantly influence these outcomes is imperative. Designing an experimental plan (vide in Table 2) to systematically vary the selected parameters and levels, potentially utilizing techniques like the Taguchi method, can optimize parameter settings and minimize the number of experimental runs required.

Figure 1. (a) EDM filled with dielectric fluid and immersed specimen (b) Specimen after machining.

Table 2. Input and their levels.

S.N.	Parameters	Level 1	Level 2	Level 3

1	Peak current (A)	9	11.5	14.5
2	Pulse-on time (μs)	50	75	100
3	Gap voltage (v)	40	45	50

Circularity (CR) and radial overcut (ROC), two output responses, were measured using a CNC coordinate measuring machine (CMM-Model: Mitutoyo CRYSTA-Apex S 9108).

Optimization by Grey Relational Analysis

By utilizing GRA to optimize machining process by considering input parameters such as circularity, MRR and radial overcut. These parameters are crucial indicators of the machining performance and quality of the components produced. The sequence of operation has been explained elsewhere [22–24]. By applying GRA, we aim to determine optimal combination of these input parameters that will result in desired output responses. In this case, the objective is to achieve the highest circularity, minimal radial overcut and maximum material removal rate, indicating precise machining with minimal waste.

RESULTS AND DISCUSSION

Mechanical and Tribological Properties

AHMMC outperformed AA7075 in both yield strength and ultimate tensile strength, according to the tensile tests shown in Table 3. While AA7075 produced yields of 76.361 MPa and 219.728 MPa, respectively, AHMMC showed yield strengths of 83.966 MPa and an ultimate tensile strength of 224.655 MPa. Fracture surface analysis indicated distinctive differences between the materials, with AHMMC exhibiting a more uniform fracture surface. These results underscore the superior mechanical properties of AHMMC compared to AA7075.

The hardness tests conducted on AHMMC and AA7075 samples revealed distinctive hardness values in Table 4. AHMMC exhibited a hardness value of 86 HRC, while AA7075 showed a hardness value of 79.3 HRC. Analysis of hardness distribution indicated variations within each material. These findings shed important light on the material's potential appropriateness for a range of applications as well as its resistance to deformation.

The wear tests conducted on AHMMC and AA7075 samples revealed distinct wear rates under similar testing conditions in Table 5. AHMMC exhibited a wear rate of 0.0001382mm^3/Nm, while AA7075 showed a wear rate of 0.0004137 mm^3/Nm. Analysis of wear mechanisms indicated variations between the materials. These results provide valuable insights into the materials' wear resistance and can inform their suitability for specific applications requiring resistance to wear and friction.

Table 3. Results of tensile test.

Specimen	Tensile stress	Yield stress
AA7075	219.728 N/mm2	76.361 N/mm^2
AHMMC	234.655 N/mm2	83.966 N/mm^2

Table 4. Results of hardness test.

S.N.	Material	Indenter (Inch)	Load (kgf)	Scale C	Hardness
1.	AA7075	1/16 (Ball indenter)	100	75	(75+83+80)/3=79.3
2.				83	
3.				80	
1.	AHMMC	1/16 (Ball indenter)	100	84	(84+89+85)/3=86
2.				89	
3.				85	

Table 5. Results of wear rate.

S.N.	Material	Wear	Wear Rate (mm^3/Nm)	Friction Coefficient
1.	AHMMC	72	0.0001382	0.233623
2.	AA7075	165	0.0004137	0.261276

Grey Relational Grade Models

Table 6 displays all experimental values' output responses. Table 7 shows result of the S/N ratio and normalization calculations made from this experimental measurement. Table 8 provides the output replies' grey relational coefficient and grey relational grade.

In general, better output answers were a reflection of grey relational grade's dominating value. It was clear from grey relational grade that input parameters such gap voltage at 45V, pulse-on duration of 50 µs, and peak current at 14.5A resulted in improved output performance.

Finding the discrete parameter's perception that influences the combined answers is essential. The key parameter for the whole process cannot be found by the optimal status result derived from a single optimization approach. Therefore, an arithmetic tool called an ANOVA was used to define the involvement of discrete factors on the multi-objective parameters and to classify the important parameter. Table 9 presents the ANOVA findings, showing that the peak current contributes the most at 53.183%, followed by the gap voltage at 7.172% and the pulse-on time at 11.528%.

The response graph Figure 2's optimal level (peak current = 14.5 A, pulse-on time = 50 µs, gap voltage = 45 V) was taken into consideration as the expected condition.

Table 6. Output responses for all the experiment.

Exp no.	Peak Current, I (A)	Pulse -on time (POT)	Gap Voltage, V	Circularity, (mm)	Radial Overcut, (mm)	Material Removal Rate (mm^3/min)
1	9	50	40	0.042	0.0897	14.788
2	9	50	45	0.023	0.132	15.481
3	9	50	50	0.033	0.1095	13.927
4	9	75	40	0.028	0.068	11.108
5	9	75	45	0.028	0.0855	11.713
6	9	75	50	0.02	0.0985	11.644
7	9	100	40	0.044	0.0845	11.551
8	9	100	45	0.033	0.082	9.016
9	9	100	50	0.031	0.094	7.6
10	11.5	50	40	0.024	0.081	22.308
11	11.5	50	45	0.026	0.1035	27.629
12	11.5	50	50	0.031	0.1045	23.64
13	11.5	75	40	0.023	0.078	19.624
14	11.5	75	45	0.03	0.095	24.724
15	11.5	75	50	0.022	0.096	20.186
16	11.5	100	40	0.024	0.1085	19.653
17	11.5	100	45	0.03	0.111	23.351
18	11.5	100	50	0.026	0.1	18.7
19	14.5	50	40	0.031	0.109	37.684
20	14.5	50	45	0.035	0.1285	44.922
21	14.5	50	50	0.025	0.1305	38.927
22	14.5	75	40	0.036	0.0995	33.307
23	14.5	75	45	0.031	0.122	36.573
24	14.5	75	50	0.039	0.1135	33.494

25	14.5	100	40	0.021	0.0935	29.955
26	14.5	100	45	0.039	0.115	35.126
27	14.5	100	50	0.019	0.1125	28.9

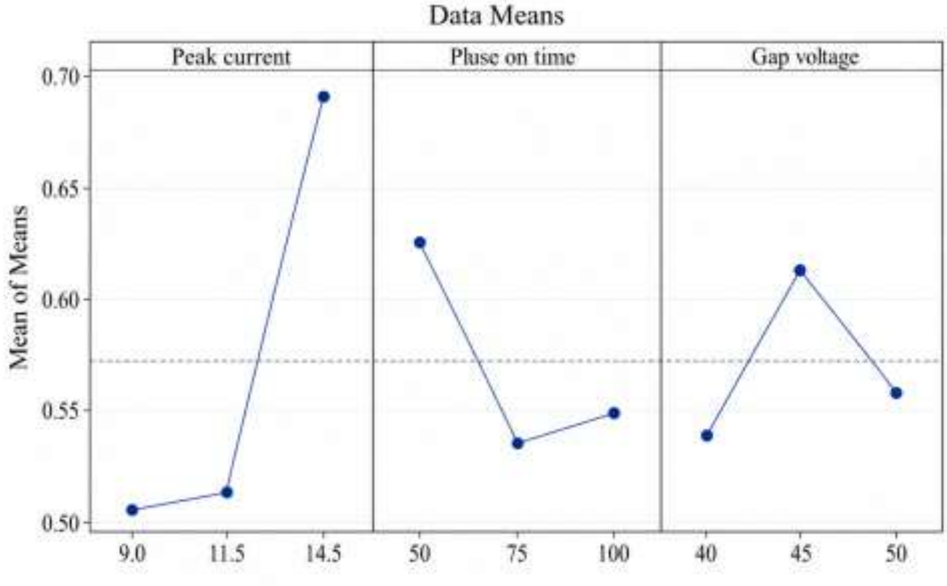

Figure 2. Main effects plot for means.

Table 7. Value of S/N ratio and normalization for all experiments.

Ex no.	CR	ROC	MRR	CR	ROC	MRR
	Calculation of S/N ratios			***Normalization of S/N ratios***		
1	27.535	20.944	-23.398	0.9446	0.4176	0.3746
2	32.765	17.589	-23.796	0.2275	1	0.4004
3	29.63	19.212	-22.877	0.6574	0.7183	0.3409
4	31.057	23.35	-20.913	0.4618	0	0.2136
5	31.057	21.361	-21.373	0.4618	0.3453	0.2434
6	33.979	20.131	-21.322	0.0611	0.5586	0.2401
7	27.131	21.463	-21.252	1	0.3275	0.2356
8	29.63	21.724	-19.1	0.6574	0.2822	0.0962
9	30.173	20.537	-17.616	0.583	0.4882	0
10	32.396	21.83	-26.969	0.2782	0.2637	0.606
11	31.701	19.701	-28.827	0.3735	0.6333	0.7264
12	30.173	19.618	-27.473	0.583	0.6478	0.6387
13	32.765	22.158	-25.856	0.2275	0.2068	0.5339
14	30.458	20.446	-27.862	0.5439	0.5041	0.6639
15	33.152	20.355	-26.101	0.1746	0.5199	0.5498
16	32.396	19.291	-25.869	0.2782	0.7044	0.5347
17	30.458	19.094	-27.366	0.5439	0.7388	0.6318
18	31.701	20	-25.437	0.3735	0.5814	0.5067
19	30.173	19.251	-31.523	0.583	0.7114	0.9011
20	29.119	17.822	-33.049	0.7275	0.9595	1
21	32.041	17.688	-31.805	0.3268	0.9828	0.9194
22	28.874	20.044	-30.451	0.761	0.5739	0.8316
23	30.173	18.273	-31.263	0.583	0.8812	0.8843
24	28.179	18.9	-30.499	0.8564	0.7723	0.8348

25	33.556	20.584	-29.529	0.1192	0.4801	0.7719
26	28.179	18.786	-30.913	0.8564	0.7921	0.8616
27	34.425	18.977	-29.218	0	0.759	0.7517

Table 8. Grade relational coefficient and grade relational grade.

Exp	CR	ROC	MRR	Grade	Rank
1	0.9003	0.4619	0.4443	0.6022	10
2	0.3929	1	0.4547	0.6159	8
3	0.5934	0.6396	0.4314	0.5548	15
4	0.4816	0.3333	0.3887	0.4012	27
5	0.4816	0.433	0.3979	0.4375	24
6	0.3475	0.5312	0.3969	0.4252	26
7	1	0.4264	0.3954	0.6073	9
8	0.5934	0.4106	0.3562	0.4534	23
9	0.5452	0.4941	0.3333	0.4576	22
10	0.4092	0.4044	0.5593	0.4577	21
11	0.4439	0.5769	0.6464	0.5557	14
12	0.5452	0.5867	0.5805	0.5708	12
13	0.3929	0.3867	0.5175	0.4324	25
14	0.523	0.5021	0.598	0.541	16
15	0.3772	0.5101	0.5262	0.4712	20
16	0.4092	0.6285	0.518	0.5186	17
17	0.523	0.6568	0.5759	0.5852	11
18	0.4439	0.5443	0.5034	0.4972	19
19	0.5452	0.634	0.8349	0.6714	6
20	0.6472	0.925	1	0.8574	1
21	0.4262	0.9667	0.8612	0.7513	3
22	0.6766	0.5399	0.7481	0.6549	7
23	0.5452	0.8081	0.8121	0.7218	5
24	0.7768	0.6871	0.7516	0.7385	4
25	0.3621	0.4902	0.6867	0.513	18
26	0.7768	0.7064	0.7832	0.7554	2
27	0.3333	0.6748	0.6682	0.5588	13

Table 9. ANOVA Table.

Source	DF	Adj SS	Adj MS	F-Value	P-Value	Contribution %
Peak current	2	0.19717	0.098585	18.91	0	53.183
Pulse-on time	2	0.04274	0.02137	4.1	0.032	11.528
Gap voltage	2	0.02659	0.013294	2.55	0.103	7.172
Error	20	0.10424	0.005212	28.116		
Total	26	0.37074				

Influence of Process Parameters on MRR

3D surface plots were developed using Minitab software, and were employed to analyze the interactive effect of independent variables such as peak current and pulse-on time, on the dependent variables namely, circularity, ROC, and MRR. Figure 3(a) illustrates the simultaneous influence of peak current (PC) and pulse-on time (POT) on material removal rate (MRR). From the surface plot, it is evident that the MRR increases slowly with an increase in pulse-on time, while it decreases for larger peak current values. The trend observed in the present study points to the fact that increased pulse duration is conducive to higher energy transfer per discharge, thus favoring efficient melting and material removal from the work surface. But in the case of a higher peak current, increased discharge energy can contribute to uneven plasma channel generation and less efficient flushing of molten material, thus decreasing net material removal rate. Therefore, the best combination to achieve the highest MRR is associated with lower peak current and longer pulse-on time, which is in good agreement with the already established optimal conditions (I = 14.5 A, POT = 50 μs, V = 45 V).

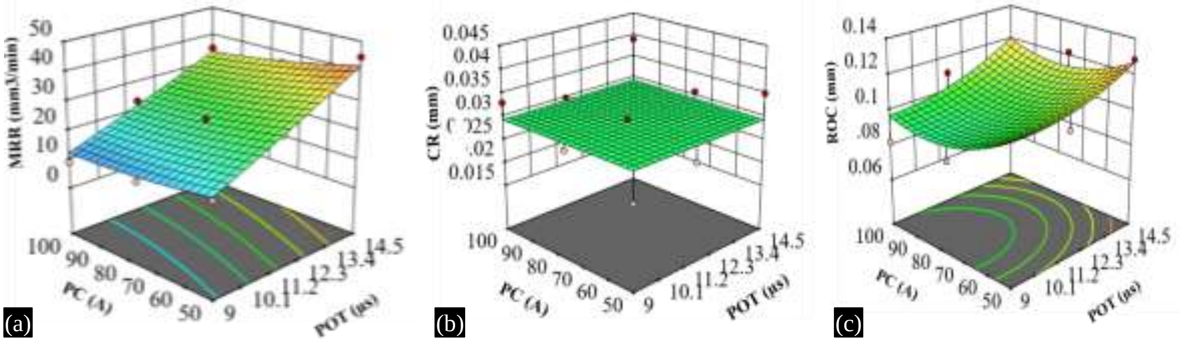

Figure 3. Effect of process parameters: (a) on MRR, (b) on circularity, and (c) radial overcut.

Effect of Circularity

Variation in circularity error as a function of peak current and pulse-on time is shown in Figure 3(b). The circularity error increases with rising peak current, whereas the impact of pulse-on time is relatively small. This rise in error can be explained by the creation of larger and irregular molten pools at higher energies of discharge, resulting in re-solidification in a non-uniform manner and geometric distortion of the drilled hole. At lower cur-rent and longer pulse-on time, the discharge energy is moderate and fairly evenly distributed, with better dimensional accuracy and lower circularity deviation.

Effect on Radial Overcut (ROC)

Figure 3(c) shows the influence of peak current and pulse-on time on the radial overcut (ROC). For increased peak current, a very high ROC was found, mainly caused by increased lateral thermal diffusion and excessive workpiece edge erosion. The use of both high current and short pulse-on time exaggerates this tendency, generating unstable discharge conditions and larger overcuts. Conversely, moderate current and extended pulse-on time provide improved control over energy delivery and flushing action, thus reducing the radial overcut.

The combined evaluation of MRR, circularity, and ROC clearly indicates a trade-off between material removal efficiency and dimensional accuracy. While an increase in pulse-on time promotes higher MRR and more stable discharge conditions, an excessive peak current adversely affects both circularity and ROC due to uncontrolled melting and uneven solidification.

CONCLUSIONS

The aluminum hybrid composite was successfully casted using stir casting approach, and was machined using EDM at different process parameters to achieve various responses. The responses were optimized using grey relational analysis tool and the obtained conclusions were listed below.

- Stir casting was used to create a hybrid aluminum composite by adding TiC and BN with a wt.% of 6 and 2.
- The base metal reinforced with 6 and 2 wt.% of TiC and BN, exhibited the highest ultimate tensile test and yield strength compared to the base metal
- From hardness and wear test results, it is concluded that the AAHMMC with 6 and 2 wt.% of TiC and BN exhibits more hardness and better wear rata as compared to AA7075.
- By using grey relational analysis, the ideal parameters, such as a peak current of 14.5 A, a pulse-on time of 50 μs, and a gap voltage of 45 V, were achieved in order to achieve minor variations in radial overcut, material removal rate, and circularity.

- The optimized parameters achieved from the response analysis were a peak current of 14.5 A, pulse-on time of 50 µs, and voltage of 45 V, corresponding to the 20th experimental condition, which implied the best combination in achieving desired performance results
- The ANOVA outputs proved that peak current had the strongest effect controlling the machining responses, with a contribution ratio of 53.183%, thus indicating its dominating influence on process behavior.
- A rise in peak current caused a significant increase in circularity error and overcut in the radial direction, while the deviation in material removal rate (MRR) became deeper under the synergistic action of increased current and reduced pulse-on time, emphasizing the precision-productivity trade-off.

REFERENCES

1. Ramesh, S., Natarajan, N., Krishnaraj, V.: Experimental investigation of Al6061/SiCp/B4Cp hybrid MMCs in wire electrical discharge machine. Indian J. Eng. Mater. Sci. 21, 409–417 (2014).
2. Siva Sankara Raju, Srinivasa Rao, G., Samantra, C.: Wear behavioral assessment of Al-CSAp-MMCs using grey-fuzzy approach. Measurement. 140, 254–268 (2019). https://doi.org/10.1016/j.measurement.2019.04.004.
3. Altinkok, N., Özsert, I., Findik, F.: Dry Sliding Wear Behavior of Al2O3 / SiC Particle Reinforced Aluminium Based MMCs Fabricated by Stir Casting Method. ACTA Phys. Pol. A. 124, 11–19 (2013). https://doi.org/10.12693/APhysPolA.124.11.
4. Vikash Kumar, K., R, S.S. raju: Statistical Modeling and Optimization of Al-MMCs Reinforced With Coconut Shell Ash Particulates. In: Deepak, B., DRK, P., and Jena, P.C. (eds.) Innovative Product Design and Intelligent Manufacturing Systems: Lecture Notes in Mechanical Engineering. pp. 703–712. Springer Nature Singapore Pte Ltd.2020, Rourkela, India (2020). https://doi.org/https://doi.org/10.1007/978-981-15-2696-1_67.
5. Kachhap, S., Singh, A., Kumar, S.: Performance evaluation of different electrode geometries in electric discharge drilling of MMCs. Int. J. Mech. Eng. Robot. Res. 8, 531–535 (2019). https://doi.org/10.18178/ijmerr.8.4.531-535.
6. Rajesh, S., Krishna, A.G., Murty, P.R., Duraiselvam, M.: Statistical Analysis of Dry Sliding Wear Behavior of Graphite Reinforced Aluminum MMCs. Eng. Technol. 6, 1110–1120 (2014). https://doi.org/10.1016/j.mspro.2014.07.183.
7. Sankara Raju, R.S., Panigrahi, M.K., Ganguly, R.I., Srinivasa Rao, G.: Optimization of tribological behaviour on Al- coconut shell ash composite at elevated temperature. IOP Conf. Ser. Mater. Sci. Eng. 314, 012009 (2018). https://doi.org/10.1088/1757-899X/314/1/012009.
8. Gangil, M., Pradhan, M.K.: Optimization the machining parameters by using VIKOR Method during EDM process of Titanium alloy. Mater. Today Proc. 5, 7486–7495 (2018). https://doi.org/10.1016/j.matpr.2017.11.420.
9. Anthony Xavior, M., Ashwath, P.: Fatigue life and Fracture Morphology of Inconel 718 machined by spark EDM process. Procedia Manuf. 30, 292–299 (2019). https://doi.org/10.1016/J.PROMFG.2019.02.042.
10. Rao, C.J., Siva Sankara Raju, R., Sreeramulu, D., Sagar, Y.: Fabrication and Evaluation of Optimized Parametric Condition During EDM Machining of Al-CSA Composite Using Taguchi Orthogonal Array. In: Lionel, G., Karthikeyan, R., and Muralidharan, V. (eds.) Advances in Design and Thermal Systems:Select Proceedings of ETDMMT 2020. pp. 411–420. Springer Singapore (2021). https://doi.org/10.1007/978-981-33-6428-8_33.
11. Alagarsamy, S. V., Raveendran, P., Ravichandran, M.: Investigation of Material Removal Rate and Tool Wear Rate in Spark Erosion Machining of Al-Fe-Si Alloy Composite Using Taguchi Coupled TOPSIS Approach. Silicon. 13, 2529–2543 (2021). https://doi.org/10.1007/S12633-020-00596-X.
12. Senthilkumar, N., Tamizharasan, T., Anandakrishnan, V.: Experimental investigation and performance analysis of cemented carbide inserts of different geometries using Taguchi based grey relational analysis. MEASUREMENT. 58, 520–536 (2014). https://doi.org/10.1016/j.measurement.2014.09.025.

13. Kumaran, S.T., Uthayakumar, M., Slota, A., Zajac, J., Thirumalai Kumaran, S., Uthayakumar, M., Slota, A., Zajac, J.: Application of Grey relational analysis in high speed machining of AA (6351)-SiC-B4C hybrid composite. Int. J. Mater. Prod. Technol. 51, 17–31 (2015). https://doi.org/10.1504/IJMPT.2015.070077.
14. Hourmand, M., Farahany, S., Sarhan, A.A.D., Noordin, M.Y.: Investigating the electrical discharge machining (EDM) parameter effects on Al-Mg2Si metal matrix composite (MMC) for high material removal rate (MRR) and less EWR–RSM approach. Int. J. Adv. Manuf. Technol. 77, 831–838 (2015). https://doi.org/10.1007/s00170-014-6491-2.
15. Kumar, R., Dhiman, S.: A study of sliding wear behaviors of Al-7075 alloy and Al-7075 hybrid composite by response surface methodology analysis. Mater. Des. 50, 351–359 (2013). https://doi.org/10.1016/j.matdes.2013.02.038.
16. Lakshmipathy, J., Kulendran, B.: Reciprocating Wear Behaviour of 7075Al/SiC and 6061Al/Al2O3 Composites : A study of Effect of Reinforcement , Stroke and Load. Tribol. Ind. 36, 117–126 (2014).
17. Selvakumar, N., Narayanasamy, P.: Optimization and Effect of Weight Fraction of MoS2 on the Tribological Behavior of Mg-TiC-MoS2 Hybrid Composites. Tribol. Trans. 59, 733–747 (2016). https://doi.org/10.1080/10402004.2015.1110866.
18. Khan, M.M., Dey, A.: Hybrid MCDM approach for examining the high-stress abrasive wear behaviour of in situ ZA-27/TiCp MMCs. Mater. Chem. Phys. 277, 125319 (2022). https://doi.org/10.1016/j.matchemphys.2021.125319.
19. Balakrishnan, M., Dinaharan, I., Palanivel, R., Sivaprakasam, R.: Synthesize of AZ31/TiC magnesium matrix composites using friction stir processing. J. Magnes. Alloy. 3, 76–78 (2015). https://doi.org/10.1016/j.jma.2014.12.007.
20. Dirisenapu, G., Dumpala, L., Pichi Reddy, S.: Parametric Optimisation of Tribological Characteristics of Novel Al7010/B 4 C/BN Hybrid Metal Matrix Nanocomposites Using Taguchi Technique. Aust. J. Mech. Eng. (2021). https://doi.org/10.1080/14484846.2021.1938940.
21. Mahesha, C.R., Deshmukh, R.G., Sunagar, P., Chandrasekaran, M., Kumar, B.S.P., Pratyush, K., Gopalan, A., Sisay, A.: Experimental Analysis on Tribological Characteristics of AZ60A/Gr/BN Magnesium Composites. J. Nanomater. 2022, 6 pages (2022). https://doi.org/10.1155/2022/2312076.
22. Raju, S.S., Rao, G.S.: Assessments of Desirability Wear Behaviour on Al- Coconut Shell Ash - Metal Matrix Composite using Grey - Fuzzy Reasoning Grade. Indian J. Sci. Technol. 10, 1–11 (2017). https://doi.org/10.17485/ijst/2017/v10i15/113826.
23. Siva Sankara Raju, R., Venkata Siva, B., Srinivasa Rao, G.: Quantitative Analysis of Tribological Performance on Al–CSA Composite Using Orthogonal Array. In: Voruganti, H.K., Kiran Kumar, K., Vamsi Krishna, P., and Xiaoliang, J. (eds.) Advances in Applied Mechanical Engineering (Lecture Notes in Mechanical Engineering (LNME)). pp. 381–388. Springer Nature Singapore Pte Ltd (2020). https://doi.org/10.1007/978-981-15-1201-8_43.
24. Rallabandi, S.R., Pilla, D.P., Dowluru, S., Palli, S., Sharma, N., Sharma, S.K., Sharma, R.C.: Critical evaluation of epoxy-hemp-pineapple-palm fiber composites using hybrid AHM-TOPSIS technique for sustainable structural applications. J. Chinese Inst. Eng. 47, 325–336 (2024). https://doi.org/10.1080/02533839.2024.2308250.

